NTNU Dept of Physics

Exam TFY4310 Molecular Biophysics 30 may 2023
Suggested solutions

Exercise 1 On hybridization of one s and two p orbitals we get:
a. three orbital in a plane.
b. two mutually perpendicular orbitals.
c. two orbitals at 180°.
d. four orbitals directed tetrahedrally.

Exercise 2. Decreasing the concentration of salt in an aqueous solution leads to
a. a decrease in the Debye screening length.
b. an increase in the Bjerrum length.
c. the weakening of electrostatic repulsions.
d. the strengthening of electrostatic attractions.

Exercise3. London dispersion forces are characterized by:
a. increasing forces between alkane ($(-CH_2-)_n$) molecules with increasing chain length (n).
b. increase with the number of double bonds for forces between molecules with alkyl chains
c. act only between apolar molecules.
d. decay with the distance between molecules according to r^{-5}.

Exercise 4. True or false statement: van der Waals interactions implies it is enthalpically favorable to move a methane (apolar) molecule from benzene (apolar) to water.
a. True. The interactions between methane and water are stronger than the interactions between methane and benzene.
b True. The water establishes more intermolecular interactions in the presence of methane than its absence.
c. True. The benzene establishes more intermolecular interactions in the presence of methane than its absence.
d. False. It is not enthalpically favorable.

Exercise 5. Two fluids are fully miscible for all mixture compositions when
a. the free energy of mixing is negative for all compositions.
b. the free energy of mixing is positive for all compositions.
c. the free energy of mixing is negative for all compositions and there is a minimum at the equimolar ratio.
d. the free energy of mixing is positive for all compositions and there is a maximum at the equimolar ratio.

Exercise 6. According to the Flory-Huggins theory, longer polymers have
a. lower conformational entropy and larger mixing entropy.
b. larger conformational entropy and larger mixing entropy.
c. lower conformational entropy and lower mixing entropy.
d. larger conformational entropy and lower mixing entropy.

Exercise 7. Which of the following sentences is **not** correct?
a. The statistical mechanical theory (SMT) of rubber elasticity assumes that the gel network has no defects.
b. To best describe the elastic contribution to the free energy of polymer gel swelling a term describing volume variation must be included in the SMT of rubber elasticity.

c. The mixing contribution of the free energy of polymer gel swelling is only valid for ideal chains.
d. When a rubber band, stretched by the action of a weight, is heated up, the band elongation decreases.

Exercise 8. Polymer networks composed of charged polymers swell more in aqueous solution than networks with neutral polymers because
a. the counterions of the polymer exert an osmotic pressure in the gel.
b. water is a poorer solvent for charged polymers.
c. there are fewer counterions inside the network than outside.
d. polyelectrolytes are more flexible than neutral polymers.

Exercise 9. Which of the following statements in the field of molecular modelling is correct?
a. Models with implicit water are well-suited to mimic hydrophobic interactions.
b. If the average quantity of a property of interest has not changed throughout a (relatively long) Monte Carlo simulation run we can safely assume that it has reached its global potential energy minimum.
c. Monte Carlo molecular modeling allows for a faster convergence (equilibration) of systems, when compared to Molecular Dynamics, due to its ability to perform unphysical moves.
d. When modeling the translational diffusion of lysozyme in aqueous solution using an atomistic model, most of the computational effort is used in moving the atoms of the protein.

Exercise 10. According to the Frank-Condon principle:
a. the relative position of the nuclei cannot be ignored during an electronic transition.
b. only fundamental vibrational transitions ($\Delta v = \pm 1$) are allowed.
c. vibrational transitions other than the fundamental are allowed if transitions between electronic states are involved.
d. the transition dipole moment needs to be zero for observing a band in IR spectroscopy.

Exercise 11
Neurodegenerative diseases are characterized by accumulation of misfolded proteins into insoluble amyloid fibrillar aggregates. One hypothesis is that intermediate structures formed by a few amyloid proteins (oligomers) are more toxic species than the mature fibrils. In this context, understanding the molecular mechanisms that govern the formation of amyloid oligomers is of large therapeutic interest, with the aim of developing effective inhibitors for the formation of these amyloid oligomers.

Several studies have reported that cell membranes can serve as common targets for amyloidogenic oligomers and three models have been proposed, as depicted in Figure 1.

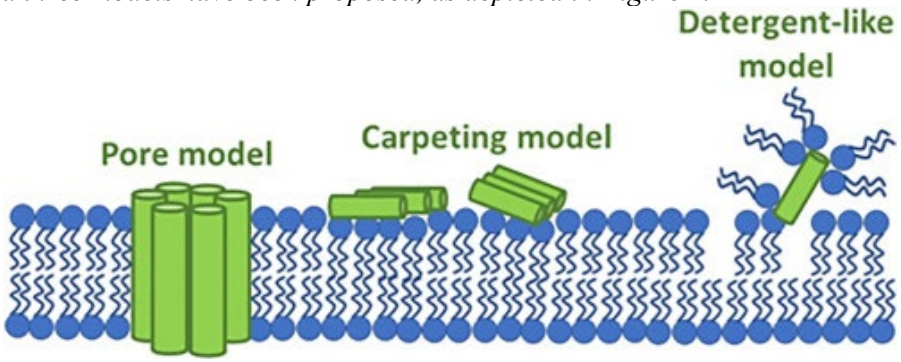

Figure 1. *Three mechanism models have been proposed to illustrate the disruption of membrane cells by interactions with amyloid proteins: Pore model, Carpeting model and Detergent-like model.*

Describe the organization of cell membrane (as illustrated in Figure 1), including a description of interactions and structural features that give rise to the planar like organization.

b) Knowing that most cell membranes are negatively charged, discuss the driving force for the association of the oligomers with the lipid membrane in the pore model and the carpeting model. The detergent-like model is named after the ability of detergent (e.g., amphiphilic molecules with one hydrocarbon chain) to disrupt lipid bilayers. Discuss the mechanism in which detergents disrupt a lipid bilayer and if the scheme in Figure 1 correctly reflects it.
Can all three models be possible for the same amyloid protein?

Suggested solution a)
The organisation of the cell membrane can be summarized as a lipid bilayer, but also with proteins in different regions in the cross-section of the lipid bilayer. This organization is adopted by lipid molecules with their amphiphilic character when blended in an aqueous solution. The organization of many lipids in the planar layer in aqueous environment is governed by:

i) The hydrophobic effect driving an assembly of the amphilic lipids with the hydrophobic tails in the interior of the membranes and hydrophilic (polar, charged) headgroups facing towards water
ii) The geometry of the individual lipid molecules in terms of a critical packing parameter not far from 1 is a further essential feature yielding stabilization of the planar phase (as opposed to e.g. a miceller, spherical geometry.

The hydrofobic effect (interactions/bonds) is connected to the fact that it is energetically favourable for water molecules to form more regular structures near apolar surfaces like the aliphatic tails of the lipids, than in free aqueous solution. This ordering, however, is entropically unfavorable. When two such apolar surfaces with structured water molecules are brought together, the apolar surfaces will not be accessible for structuring of water molecules, and thus, a larger fraction of the water is not stuctured. Or in other words: the association of the apolar surfaces is driven by an entropy gain of the water molecules not any longer ordered by apolar surfaces now in proximity with other apolar surfaces

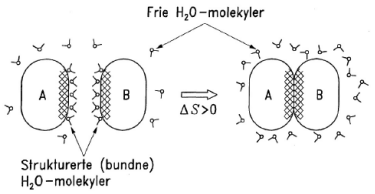

Schematic illustration of entropy gain of water occurring on association of apolar surfaces

The organization of amphiphilic lipids in preferred planar structures, as in cell membranes, as opposed to e.g. micellar geometries is affected by the structure of lipids in terms of number and length of aliphatic tails attached to each headgroup and also in view of the size of the headgroup. This is rationalized in terms of the parameter "critical packing parameter" (CPP)

The CPP of lipids with one aliphatic tail is usually significantly less than 1, giving rise to a micellar / spherical geometry of the assembled lipids (at not too high lipid fraction, but still significant beyond that required to form the assembled structures). The lipids with two aliphatic tails adopt a more planar geometry of the assembled structures as their CPP is closer to 1 than for the 1 aliphatic tail lipids.

Overall, this give the organization in the lipid bilayer by polar headgroups of lipids facing towards water phase (both intra and extracellular) and tail (lipophilic) towards the interior in the double layer.

Suggested solution b)

For amyloid proteins to assemble as transmembrane structures giving an overall central pore in the cylinder like overall structure, each protein should have regions on their surface that favour the diverse interactions/medium in the different regions:

For the cylinder surface when modelling individual amyloid proteins as cylinders: A part of that surface preferentially interacting with the lipohilic part internally in the cell membrane.

Another part of the cylinder surface: facing towards the pore channel. Since this is connected to aquous phase outside the cell membrane, this part should then be hydrophilic.

Another part of the cylinder like surface: mediating interactions between the amyloid proteins aling the cylinder: a surface

The end of the cylinders: hydrophilic (to avoid getting internalized in the lipophilic domain of the cell membrane. Due to the negative charge of the membrane: the end of the amyloid cylinder like model should not be cationic; it can be anionic / or carry both type of charges

In the carpet model,. there are interactions between the indivudal proteins along their cylinder surface as well as interaction between the aggregated protein and the negatively charged headgroups. Mechanistic in the latter: of electrostatic nature between e.g. cationic groups on the amyloid surface and anionic headgroups (also having an entropic contribution associated with counterion release for the oppositely charged components). A possible mechanism for the stability of the aggregated proteins in the carpet model: hydrophobic domains along at least part of the cylinder length; but limited to a sector so another sector / or stripe along the cylinder can mediate the interaction to the lipid headgroups. Another possibility for the lateral association: localized interaction sites e.g. charged groups, opposite, along the cylinders.

In the detergent model: the interaction between the negatively charged lipid headgroups and the undividual proteins are likely to be dominated by electrostatic mechanism. (anion headgroup – cationic groups on the protein – almost everywhere. The potential energy of the protein – lipid aggregate in the detergent model must drive the lipids from the membrane to prefarably interact with the protein.

It is difficult to reconsile the three possible models for aggregation and interaction within the same amyloid since the required distribution of domains for protein aggreation and interaction with the membrane are different for the three models.

Exercise 12

Figure 1 shows a 1H NMR spectrum of a molecule. This is shown as chemical shift relative to a reference (but the signal for the reference is not shown). The numbers shown near the peaks in the spectrum indicate the relative integral of the area under the various peaks.

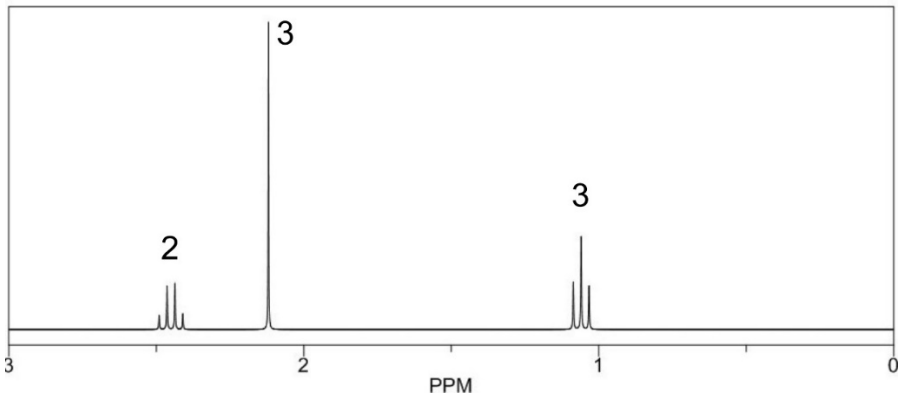

Describe which principles are used as a basis for interpreting such 1H NMR spectra. Which molecule has given rise to the spectrum shown?

Suggested solution:

The principles underpinning interpretation of proton NMR spectra are:

Absolute value of shift

Relative area under the peaks - The relative area under the absorption peaks in the different groups tells us the relative number of protons within each of the three groups.

Splitting of the peaks (fine structure): the splitting of the peaks is due to spin-spin coupling between the nuclei (protons in this case) and of the respective groups and protons in a neighbouring group.

Applying these principles offers clue of the actual molecule as follow:
From the spectrum, we observe three groups of absorption peaks where the shift, relative area and fine structure are as follow (and there is introduced a notation).

Shift	1.1	2.2	2.4
Relative area	3	3	2
# peaks/	3	1	4
Notation	A	B	C

It is assumed that the backbone is carbon.
For peak B: Since there are no splitting of this, it means that there are no protons on the carbon (or other atoms neighbouring) the carbon binding the proton(s) with resonance at 2.2

The splitting of the peaks is due to spin-spin coupling between a nucleus (proton in this case) and the protons in a neighbouring group. In the case of the group A, there is three peaks. This indicate that the number of equivalent nearest neighbour protons is two, which gives rise to a multiplet with three peaks (triplet) with relative area
1 : 2 : 1 = (↑↑) : (↑↓, ↓↑) : (↓↓).

For the group C, there is an observation that this is split in 4, indicating that the number of nearest neighbour protons is three giving rise to a quadruplet with relative area
1 : 3 : 3 : 1 = (↑↑↑) : (↑↑↓, ↑↓↑, ↓↑↑) : (↓↓↑, ↓↑↓, ↑↓↓) : (↓↓↓).

To summarize:

A: relative area 3, nearest neighbor protons: 2
B: relative area 3, nearest neighbor protons: 0
C: relative area 2, nearest neighbor protons: 3

Thus, structures

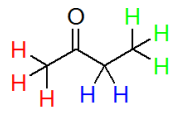

or CH3 - O - CH2 -CH3; where(A: Green; B: red, C: blue)

satisfy the relative areas and splitting of the peaks.

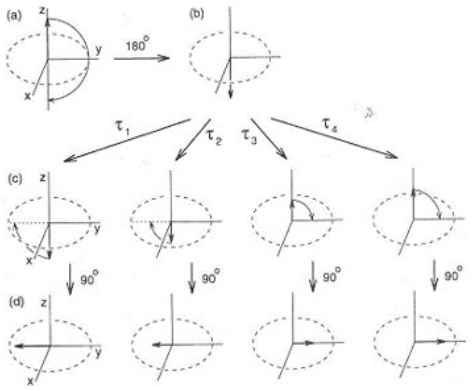

Figure 2 illustrates changes in net magnetization of a sample occurring in a pulse sequence for determining one of the two relaxation mechanisms in NMR. The different parameters τx, x=1,2,3,.. are characterized by τ1 < τ2 < τ3 < τ4 and the effect of these different values is illustrated by the different subfigures.

Briefly describe the two relaxation mechanisms that occur in NMR.
Describe the pulse sequence in Figure, which changes occur in the net magnetization at the various steps in the pulse sequence, which net magnetization is determined, and which relaxation parameter is determined by the pulse sequence

Suggested solution.
The two relaxation mechanism in NMR is the spin-lattice (T1), or longitudinal; and spin-spin (T2) relaxation.
Spin-lattice (T_1) relaxation: Re-equilibration of the populations of spins in the lowest and higher energy levels by transfer to thermal motion.
T_1 is a measure of the time it takes random processes to establish the equilibrium value Mz in a simple first-order fashion as a function of time, after $\boldsymbol{B}_z$ is turned on/off.

Spin-spin (T_2) relaxation: Interaction of spins with other spins in the sample leading to the unbundling of spins in the xy-plane. Does not involve the flipping of spins between levels
Possible illustration:

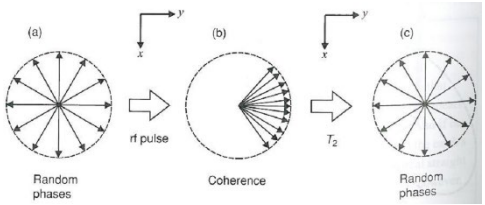

Spontaneous first-order process, characterised by T_2:

$$M_x = M_{x,0}(t)\exp^{-t/T_2}$$
$$M_y = M_{y,0}(t)\exp^{-t/T_2}$$

Figure 2 illustrate a 180º-preparation – 90º pulse sequence in an inversion recovery method to determine the spin-lattice relaxation time. In the graph (e) below, the preparation phase has the duration , τ, with the specific examples of this duration as illustrated in the graph.

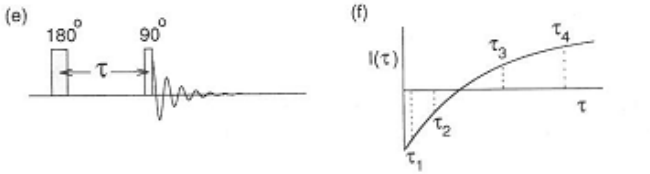

In the first step, transition from a) to b), the net magnetization initially along the positive z-axis is given a 180º pulse inducing a flipping of the net magnetization to be of the same magnitude, but pointing in the negative z-direction (end point of the pulse is illustrated in b).

During the preparative phase, the net magnetization (along the z-axis) is reduced due to the spin-lattice relaxation mechanism. After a certain duration of this phase, e.g., $\tau 1$ the sample is exposed to a 90º pulse inducing a flip the net magnetization to be in the x-y plane; and thereby being detectable to the receiver coil. Thus, the actual magnitude of the net magnetization after the preparative phase is determined. After allowing ample time for the system to restore equilibrium (same as net magnetization as in fig 2a), the sequence is repeated many times for each value of τ, yielding a signal relaxation curve as indicated in the above fig (f). This is the basis for determination of the T1 parameter

Exercise 13

The Lamm equation and the definition of the sedimentation coefficient are central to the hydrodynamically based determination of properties of biological macromolecules (biomolecules) in solution by centrifugation (sedimentation).

Describe two different analysis strategies for quantitative (analytical) determination of properties of biomolecules based on data obtained by velocity sedimentation. The description should include a brief description of how the experiment is carried out, what is observed, which equations are used as a basis and further assumptions / deductions used for the relevant (parts) of data that are analyzed, and which quantitative data is obtained.

Suggested solution.
In analytical centrifugation, also referred to as analytical ultracentrifugation (AUC) one can either use sedimentation velocity or equilibrium centrifugation.Here, it is the sedimentation velocity approach that is used for both analysis strategies. Such experiments are conducted by loading the sector like sample cell with the macromolecule sample to yield an initially distance (r) independent concentration profile.

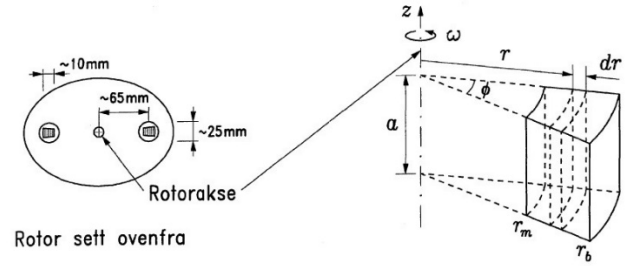

Fig. , A rotor used in AUC seen from the top (left) and the sector like sample cell.
The sample is located between a distance rm and rb (meniscous and bottom) from the rotational axis within the sector like sample cell. It is assumed that the instrument is equipped with a device providing the concentration of the sample for r between rm and rb (e.g. absorbance based).
The experiments are conducted:

Sedimentation velocity: at a rather high revolution rate yielding migration of the concentration gradient initially at the meniscous towards the bottom, and depletion (reduction of the concentration in a plateau region):

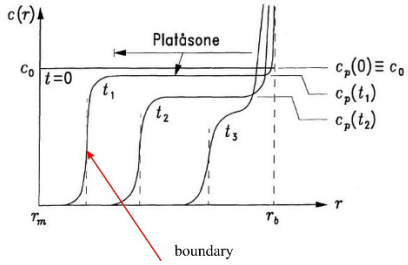

Fig. Schematic illustration of concentration profiles between rm and rb observed in AUC conducted to use sedimentation velocity as the analysis strategy. The concentration profiles are illustrated at the

start of the centrifugation (t=0) and for increasing duration of the centrifugation at constant ω ($t_3 > t_2 > t_1 > 0$). The characteristic moving boundary of the concentration profile towards larger r with increasing duration of the centrifugation and the plateau region is depicted.
The sedimentation velocity experiments can used to estimate quantitative information on biopolymer parameters based on the Lamm – eq:

$$\frac{\partial c(r,t)}{\partial t} = D_T\left(\frac{\partial^2 c(r,t)}{\partial r^2} + \frac{1}{r}\frac{\partial c(r,t)}{\partial r}\right) - s\omega^2\left(r\frac{\partial c(r,t)}{\partial r} + 2c(r,t)\right)$$

Where: $c(r,t)$ is the concentration (as function of radial position and time)

D_T is the translational diffusion coefficient.

s is the sedimentation coefficient given by: $s = u/\omega^2 r$, where u is the sedimentation velocity and ω the angular velocity of the rotor.
The sedimentation coefficient can be determined using the data from plateau region where c(r,t) is nearly independent of r. This is method 1 here. In this region. Due to the assumption that c(r,t) is independent on r, one gets:

$$\frac{\partial c_p(r,t)}{\partial r} = 0 \text{ and } \frac{\partial^2 c_p(r,t)}{\partial r^2} = 0$$

where the subscript p has been introduced to denote that this is the plateau region. Inserting this in the Lamm eq yields:

$$\frac{\partial c_p(t)}{\partial t} = -2s\omega^2 c_p(r,t)$$

Integrating this eq yields: $c_p(t) = c_0 \exp\left(-2s\omega^2 t\right)$

Solving for the sedimentation coefficient yields a working expression for obtaining the value of s from experimental data:

$$s = \frac{\ln\left(c_0/c_p(t)\right)}{2\omega^2 t}$$

The other method is the moving boundary method, where the definition of the sedimentation coefficient is used and u is extracted from the the position of the moving boundary:

$$s = \frac{u}{\omega^2 r} \approx \frac{d\overline{r}/dt}{\omega^2 \overline{r}} = \frac{d\ln(\overline{r})}{\omega^2 dt}$$

In this eq, the parameter $\overline{r}$ depict the location of the peak of dc/dr in the moving boundary.
The sedimentation coefficient is a molecular parameter.
It nevertheless can be combined with the diffusion coefficient to obtain the molar mass:

$$M = \frac{s\,k_B T N_A}{D_T(1-\overline{V}^{(S)}\rho_0)}$$

Exercise 14

Proteins typically show a ratio between absorption of light at wavelengths of 280nm and 260nm, respectively, to be A280/A260 = 2. For DNA and nucleotides, this ratio is A280/A260 = 0.5.
A purified ATP-binding protein with a molecular extinction coefficient ε280 = 12,000 M-1 cm-1 is checked for the possible content of ATP. A solution with this protein is characterized in a spectrophotometer where the path length of light in the sample is 1 cm, and absorption at 280 and 260 nm is determined to be A280 = 0.5 and A260 = 0.35 respectively.
What is the proportion of ATP (or ADP) in relation to the protein? The molecular extinction coefficient for ATP at 260 nm is ε260 = 15,000 M-1 cm-1.

Suggested solution:

In the solution being characterized there can be both protein and ATP (linked to the protein). Indicates the concentrations of these with c_p and c_{ATP}. Absorption measured at the two wavelengths can come from both the protein and ATP

$$A_{280} = c_p \varepsilon_{280}^{p} l + c_{ATP} \varepsilon_{280}^{ATP} l$$

$$A_{260} = c_p \varepsilon_{260}^{p} l + c_{ATP} \varepsilon_{260}^{ATP} l$$

where l is the pathlength. In the notation used here, p or ATP is also used in superscript to indicate the molecular extinction coefficient component

.

Base don the information: ε_{280}^{p} =12000 M^{-1} cm^{-1}; ε_{260}^{p} =6000 M^{-1} cm^{-1};

ε_{280}^{ATP} =7500 M^{-1} cm^{-1}; ε_{260}^{ATP} =15000 M^{-1} cm^{-1};

The set of eq including observed data is then given:

$$0.5 = 12000\,\mathrm{M}^{-1} c_p + 7500\,\mathrm{M}^{-1} c_{ATP}$$

$$0.35 = 6000\,\mathrm{M}^{-1} c_p + 15000\,\mathrm{M}^{-1} c_{ATP}$$

When this is solved (for example by multiplying the first by 2 and subtracting the second; or direct insertion), we get::

c_p = 36 µM and c_{ATP} = 8.9 µM.

The fraction of ATP relative to protein is 0.25 (25%); or: ¼ of the proteins in the sample has on average ATP bound.

Exercise 15

Density gradient centrifugation has been run until equilibrium for a sample that can contain both double-stranded (double helix) and single-stranded DNA. The density of the solvent (unit: g/cm3) depends on the distance r (given in unit: cm) from the rotor axis given by:

$$\rho(r) = 1.87 \exp\left(\frac{2}{12 - r^2}\right)$$

Equation 1 is valid for r between the meniscus, rm=5 cm, and the bottom of the sample cell, rb = 7 cm.

Calculate the position in the sample cell in relation to the meniscus for double-stranded DNA with =0.617 ml/g and single-stranded DNA with = 0.574 ml/g.

Suggested solution:

The position of a macromolecule with a given partial specific volume after centrifugation to equilibrium will be the location where there is no net force acting on the macromolecule. Or in other words, the sedimentation coefficient will be 0. Using the Svedberg equation:

$$s_i = \left(1 - \overline{V}_i^{(S)} \rho_0\right)$$

where the index i is for the actual molecule, $\overline{V}_i^{(S)}$ is the partial specific volume of the macromolecule, and ρ_0 is the density of the solvent.

Using the condition that s is 0; thus yielding: $1 = \overline{V}_i^{(S)} \rho_0$

and inserting for the distance dependent density, one gets:

$$1 = \overline{V}_i^{(S)} \rho_0 = \overline{V}_i^{(S)} 1.87 \exp\left(\frac{2}{12 - r^2}\right)$$

For the single stranded DNA, inserting $\overline{V}_{ssDNA}^{(S)}$ = 0.574 ml/g yields:

$$1 = 0.574 \cdot 1.87 \exp\left(\frac{2}{12 - r^2}\right); \quad \frac{2}{12 - r^2} = -7.08 \cdot 10^{-2};$$ r in cm.

This gives: the position for the ssDNA from the rotor axis: 6.34 cm (the negative r value also being a solution to the equation has no physical meaning).
The position of the ssDNA from the meniscous is this: r(ssDNA)-r_m = 1.34 cm
For the dsDNA: using the same approach as for the dsDNA, the numerical solution yields r(dsDNA) = 5.10 cm. This correspond to a distance 0.10 cm from the meniscous

Exercise 16

Light scattering measurements were performed on a solution of a oligomeric protein formed by four subunits. By analysing a Zimm plot we could obtain lines extrapolated to zero concentration for the intact protein and for the subunits dissociated. It is observed a slope of the line c = 0 for the intact protein that is four times larger than the corresponding dissociated (individual) subunits. What is the most probable structure for the protein, a spherical tetrahedral system or a linear system of the four subunits. Suppose that in both cases the subunits are identical and with spherical symmetry? Consider that the radius of gyration of the spherical and linear tetramers are, respectively, 2rG and 4rG, where rG is the radius of gyration of each monomer subunit.

Suggested solution:
The Zimm equation:

$$\frac{\kappa c}{R_\theta} = \frac{1}{M}\left[1 + \frac{16\pi^2}{3\lambda^2} R_G^2 \sin^2\theta/2\right]\left[1 + 2B_2 c\right]$$

where

κ is an optical constant :

R_θ is the Rayleigh ratio – related to the determined mean field intensity and polarization of incident light

c is the concentration

M: is the molar mass

λ : is the wavelength of light in the solution

R_G is the radius of gyration

θ is the scattering angle

B_2 is the second virial coefficient

In the limit of zero concentration of the molecules, the Zimm eq simplifies to:

$$\left.\frac{\kappa c}{R_\theta}\right|_{c=0} = \frac{1}{M}\left[1 + \frac{16\pi^2}{3\lambda^2} R_G^2 \sin^2\theta/2\right]$$

Thus, there will be slope conventionally implemented as $\kappa c/R_\theta$ versus $\sin^2\theta/2 + Ac$ (where A is a constant), will reduce to $\kappa c/R_\theta$ versus $\sin^2\theta/2$ at c = 0. The slope at c=0 of the Zimm plot:

$$\text{slope}\big|_{c=0} = \frac{1}{M}\frac{16\pi^2}{3\lambda^2} R_G^2 = const\,\frac{1}{M} R_G^2$$

For the subunits (monomer): radius of gyration r_G and molar mass: $M = M_{mono}$

$$\text{slope}\big|_{c=0} = const\,\frac{1}{M_{mono}} r_G^2$$

For tetrahedral geometry of the subunits

radius of gyration $2r_G$ and molar mass: $M = 4M_{mono}$

$$\text{slope}\big|_{c=0} = const\,\frac{1}{4M_{mono}}\left(2r_G\right)^2 = const\,\frac{1}{M_{mono}} r_G{}^2$$

For linear geometry of the subunits

radius of gyration $4r_G$ and molar mass: $M = 4M_{mono}$

$$\text{slope}\big|_{c=0} = const\frac{1}{4M_{mono}}\left(4r_G\right)^2 = const\frac{1}{M_{mono}}4r_G{}^2$$

Thus, the calculations indicate that organisation of the monomers in a linear geometry is the one that is in agreement with the given experimental observation